

Influence of intramolecular hydrogen bond formation sites on fluorescence mechanism

Hong-Bin Zhan(战鸿彬), Heng-Wei Zhang(张恒炜), Jun-Jie Jiang(江俊杰), Yi Wang(王一), Xu Fei(费旭), and Jing Tian(田晶)

Citation: Chin. Phys. B, 2022, 31 (**3**): 038201. DOI: 10.1088/1674-1056/ac29ad

Journal homepage: http://cpb.iphy.ac.cn; http://iopscience.iop.org/cpb

What follows is a list of articles you may be interested in

Theoretical investigation of fluorescence changes caused bymethanol bridge based on ESIPT reaction

Xinglei Zhang(张星蕾), Lixia Zhu(朱丽霞), Zhengran Wang(王正然), Bifa Cao(曹必发), Qiao Zhou(周悄), You Li(李尤), Bo Li(栗博), Hang Yin(尹航), and Ying Shi(石英)

Chin. Phys. B, 2021, 30 (**11**): 118202. DOI: 10.1088/1674-1056/abf131

Relationship between ESIPT properties and antioxidant activities of 5-hydroxyflavone derivates

Chaofan Sun(孙朝范), Bifa Cao(曹必发), Hang Yin(尹航), Ying Shi(石英)

Chin. Phys. B, 2020, 29 (**5**): 058202. DOI: 10.1088/1674-1056/ab7ea1

Theoretical study on the relationship between the position of the substituent and the ESIPT fluorescence characteristic of HPIP

Xin Zhang(张馨), Jian-Hui Han(韩建慧), You Li(李尤), Chao-Fan Sun(孙朝范), Xing Su(苏醒), Ying Shi(石英), Hang Yin(尹航)

Chin. Phys. B, 2020, 29 (**3**): 038201. DOI: 10.1088/1674-1056/ab6d50

Exploring the effect of aggregation-induced emission on the excited state intramolecular proton transfer for a bis-imine derivative by quantum mechanics and our own *n*-layered integrated molecular orbital and molecular mechanics calculations

Huifang Zhao(赵慧芳), Chaofan Sun(孙朝范), Xiaochun Liu(刘晓春), Hang Yin(尹航), Ying Shi(石英)

Chin. Phys. B, 2019, 28 (**1**): 018201. DOI: 10.1088/1674-1056/28/1/018201

Effect of intramolecular and intermolecular hydrogen bonding on the ESIPT process in DEAHB molecule

Hui Li(李慧), Lina Ma(马丽娜), Hang Yin(尹航), Ying Shi(石英)

Chin. Phys. B, 2018, 27 (**9**): 098201. DOI: 10.1088/1674-1056/27/9/098201

Influence of intramolecular hydrogen bond formation sites on fluorescence mechanism

Hong-Bin Zhan(战鸿彬)[1], Heng-Wei Zhang(张恒炜)[1], Jun-Jie Jiang(江俊杰)[1], Yi Wang(王一)[1,†], Xu Fei(费旭)[2], and Jing Tian(田晶)[1]

[1] *School of Biological Engineering, Dalian Polytechnic University, Dalian* 116034, *China*
[2] *Laboratory Analyst of Network Information Center, Dalian Polytechnic University, Dalian* 116034, *China*

(Received 23 July 2021; revised manuscript received 22 August 2021; accepted manuscript online 24 September 2021)

The fluorescence mechanism of HBT-HBZ is investigated in this work. A fluorescent probe is used to detect HClO content in living cells and tap water, and its structure after oxidation by HClO (HBT-ClO) is discussed based on the density functional theory (DFT) and time-dependent density functional theory (TDDFT). At the same time, the influence of the probe conformation and the proton transfer site within the excited state molecule on the fluorescence mechanism are revealed. Combined with infrared vibrational spectra and atoms-in-molecules theory, the strength of intramolecular hydrogen bonds in HBT-HBZ and HBT-ClO and their isomers are demonstrated qualitatively. The relationship between the strength of intramolecular hydrogen bonds and dipole moments is discussed. The potential energy curves demonstrate the feasibility of intramolecular proton transfer. The weak fluorescence phenomenon of HBT-HBZ in solution is quantitatively explained by analyzing the frontier molecular orbital and hole electron caused by charge separation. Moreover, when strong cyan fluorescence occurs in solution, the corresponding molecular structure should be HBT-ClO(T). The influence of the intramolecular hydrogen bond formation site on the molecule as a whole is also investigated by electrostatic potential analysis.

Keywords: benzothiazole, excited state intramolecular proton transfer, fluorescence mechanism, density functional theory

PACS: 82.39.Jn, 31.15.ee, 87.15.A– **DOI:** 10.1088/1674-1056/ac29ad

1. Introduction

Hypochlorous acid (HClO) is a weak acid with oxidizing properties, biosynthesized by hydrogen peroxide (H_2O_2) and chloride ions (Cl^-) in the presence of myeloperoxidase (MPO).[1] As a powerful bactericidal agent in the natural immune system during pathogen invasion, the HClO often plays a crucial role in the immune defense system of living organisms. However, the disruption of the balance of HClO in the organism often leads to many diseases, such as cardiovascular diseases,[2] inflammatory diseases,[3] certain cancers,[4] and neurodegenerative diseases.[5] Therefore, it is essential to pay attention to the HClO levels in organisms to better understand the physiological and pathological functions of living cells.

Compared with traditional analytical techniques, the synthesized probe-based fluorescence imaging has become a powerful tool for the detection of HClO in and out of organisms due to its unique advantages such as high sensitivity, spatial and temporal resolution, simple operation, and real-time imaging.[6–12] As is well known, the 2-(benzothiazol-2-yl)-phenol (HBT) group is a compound with excellent excited-state intramolecular proton transfer (ESIPT) properties.[13–17] The HBT and its derivatives can produce ESIPT tautomers (keto-form) that can exhibit fluorescence emissions at longer wavelengths than the enol form.[18–21] Based on the HBT moieties and their derivatives, fluorescent probes for hypochlorite detection in organisms have already been designed and synthesized. The low toxicity fluorescent probes of detecting HClO in tap water, exogenous HClO in Hela cells using the specific reaction of hypochlorous acid (HClO) with azo-phenyl have been synthesized.[22] Recently, a benzothiazole-based fluorescent probe, HBTD-V, has been reported.[23] It can sensitively respond to viscosity changes in biological systems and has shown successfully image viscosity changes in living MCF-7 cells, mouse lung organs and tissues, and in vivo in live mice. However, the mechanisms of some fluorescent probes have not been explained in detail, and a better understanding of the mechanisms by which fluorescent probes work can help researchers design stable and efficient probes more quickly and accurately. Therefore, it is crucial to investigate the mechanism of action of hypochlorite fluorescent detection probes in organisms.

So far, the mechanisms of a huge number of fluorescent probes are based on the ESIPT or intramolecular charge transfer (ICT) mechanisms.[24–29] Under photoexcitation conditions, these fluorescent probes often have large Stoke shifts [30–36] and can effectively reduce the interference of autofluorescence.[37] Thus, a large number of ESIPT fluorescent probes to detect HClO content in organisms have been designed and synthesized. An HClO detection probe (HBT-HBZ), which can be used to detect HClO levels in liv-

†Corresponding author. E-mail: wangyi@dlpu.edu.cn
© 2022 Chinese Physical Society and IOP Publishing Ltd

ing cells and tap water,[38] has been synthesized (scheme 1 in Fig. 1). The HBT-HBZ emits a faint orange fluorescence when a small amount of HClO is in the system, and at the same time, it will immediately undergo an intramolecular cyclization reaction with HClO converting bridgeless C=N into bridging C=N. After the reaction, the newly generated substance, named HBT-ClO, can exhibit an intense cyan fluorescence. Although the conversion process of HBT-HBZ into HBT-ClO was revealed, the mechanism of luminescence of HBT-HBZ and HBT-ClO in solution has not been clarified. The sensing mechanism of fluorescent probes is the key to the development of fluorescent probes. To explore the sensing mechanism of fluorescent chemical sensors, the quantum chemical computational methods are used, which can provide comprehensive photophysical processes and data.[39–42]

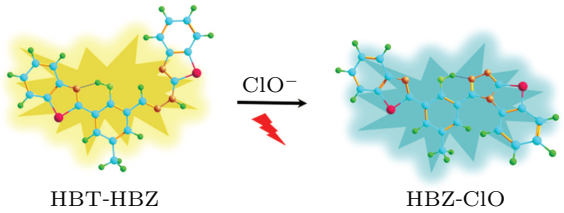


Fig. 1. Scheme 1: Illustrating mechanism of HBT-HBZ fluorescent probe proposed in the experiment.[38]

In this paper, theoretical calculations will be used to elucidate the fluorescence mechanism of HBT-HBZ and HBT-ClO and the corresponding isomers in detail. By plotting the potential energy curves and analyzing frontier molecular orbitals (FMOs), the reasons why HBT-HBZ and HBT-ClO and their isomers exhibit single fluorescence properties in water and the corresponding molecular structures when strong cyan fluorescence phenomena occur, will be explained in detail. The influence of the intramolecular hydrogen bond formation site on the molecule as a whole is also investigated through the electrostatic potential analysis.

2. Computational details

In this study, all the theoretical calculations were based on the Gaussian16 software.[43] The ground (S_0) state and excited (S_1) state were fully optimized using the density functional theory (DFT) and time-dependent DFT (TD-DFT) with range separated Becke's three-parameter hybrid exchange function with Lee–Yang–Parr gradient-corrected correlation (B3LYP) functional.[44] The triple-ζ valence quality with one set of polarization functions (TZVP) basis set was adopted.[45] In order to make the calculation results more consistent with the experimental requirements,[46] we considered the solvation effect (water) by using the integral equation formalism variant of the polarizable continuum model (IEFPCM).[47,48] The D3 version of Grimme's dispersion was included to account for the dispersion forces.[49] The Multiwfn software[50,51] was used to make better analysis.

Generally speaking, the most commonly used method to predict the reaction rate constant k (in unit s^{-1}) is Eyring's transition state theory (TST), which can be written in a form based on a partition function and a form based on thermodynamic quantities. For the latter, the reaction rate constant k (in unit s^{-1}) is directly determined by the free energy barrier. Therefore, most of reaction rate constants are based on the form of thermodynamic quantities. The TST can be rewritten as an equivalent thermodynamic form as follows:[52]

$$k^{\mathrm{TST}} = \sigma \frac{k_{\mathrm{B}}T}{h} \left(\frac{RT}{P_0}\right)^{\Delta n} \mathrm{e}^{-\Delta G^{0,\neq}/(k_{\mathrm{B}}T)}.$$

Standard activation free energy is as follows:

$$\Delta G^{0,\neq}(T) = G^{0}_{\mathrm{TS}}(T) - G^{0}_{\mathrm{Reactant}}(T),$$

$\sigma_{\mathrm{rot,R}}$ and $\sigma_{\mathrm{rot,TS}}$ are the rotation coefficients of reactants and transition states, and are related by[53]

$$\sigma = \frac{\sigma_{\mathrm{rot,R}}}{\sigma_{\mathrm{rot,TS}}},$$

generally $\sigma = 1$.

3. Results and discussion

The geometric structures of HBT-HBZ and HBT-ClO are shown in Figs. 2(a) and 2(c). It can be found that in HBT-HBZ, C–C single bonds and N=N double bonds can be rotated in the imine side-chain group adjacent to the hydroxyl group. To ensure the imine group can still be oxidized by HClO to generate triazole groups after the molecular structure has been twisted, the C_7–C_8 single bond is twisted as shown in Fig. 2(b), named HBT-HBZ(T). For HBT-ClO, when an intramolecular hydrogen bond is formed between the hydroxyl group and triazole group, the isomer of HBT-ClO can be obtained as shown in Fig. 2(d), named HBT-ClO(T). The bond length and bond angle parameters of HBT-HBZ and HBT-ClO and their isomers are shown in Table 1. The O_1–H_2 bond lengths of the four molecules increase from 0.996, 0.997, 0.998, and 0.986 Å (S_0) to 1.034, 1.038, 1.064, and 1.022 Å (S_1), and the bond lengths of the $H_2\cdots N_3$ shorten from 1.696, 1.682, 1.697, and 1.804 Å (S_0) to 1.563, 1.546, 1.498, and 1.604 Å (S_1), respectively. Thus, the intramolecular hydrogen bond (O_1–$H_2\cdots N_3$) tends to be strengthened in S_1 state, which is favorable for the ESIPT process. The structural parameters of the dihedral angle are shown in Table S1 (see supplementary information).

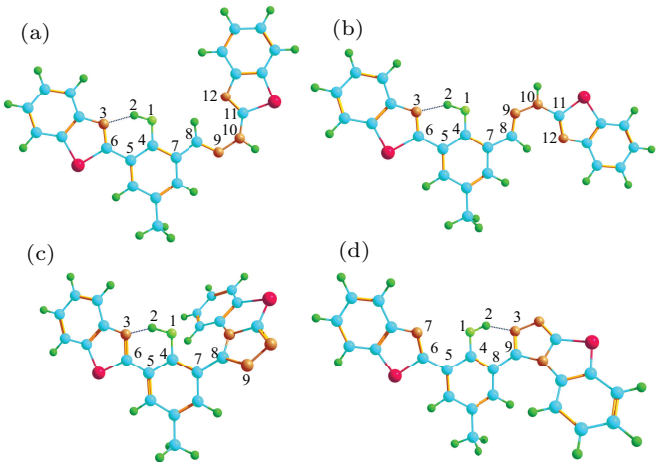


Fig. 2. Structures of (a) HBT-HBZ, (b) HBT-HBZ(T), (c) HBT-ClO, and (d) HBT-ClO(T) in water samples. Carbon atoms are cyan, hydrogen atoms are green, oxygen atoms are light green, nitrogen atoms are golden, and sulfur atoms are pink.

To better characterize the optical properties of HBT-HBZ and HBT-ClO and the corresponding isomers, the absorption (Abs.) spectra and emission spectra are shown in Fig. 3 and Table 2, where K means the structure after proton transfer. It can be seen that the absorption peaks of HBT-HBZ and HBT-HBZ(T) are located at 400 nm and 388 nm, and the fluorescence (Flu.) peaks are located at 483 nm and 467 nm, respectively, and the fluorescence peaks after proton transfer (Flu·K) are located at 623 nm and 596 nm, respectively. For HBT-ClO and HBT-ClO(T), the absorption peaks are located at 350 nm and 341 nm, the fluorescence peaks are located at 430 nm and 422 nm, respectively, and the fluorescence peaks after proton transfer are located at 553 nm and 574 nm. Interestingly, only the single fluorescence peaks at 572 nm and 470 nm are measured for HBT-HBZ and HBT-ClO in the experiment. Furthermore, in the experiment, for HBT-HBZ, the fluorescence peaks are consistent with the keto-structure spectra after proton transfer; and for HBT-ClO, the fluorescence peaks are in good agreement with the enol-structure spectra. Comparing with the fluorescence spectrum, strong fluorescence property of HBT-ClO(T) is exhibited in the enol-structure. Thus, in the experiment, the strong cyan fluorescence should be emitted from the HBT-ClO(T) structure.

Table 1. Values of bond length (in unit Å) and bond angle (°) of HBT-HBZ, HBT-HBZ(T), HBT-ClO, and HBT-ClO(T) in S state and S_1 state, (K) corresponds to the keto-structure after ESIPT process.

	States	O_1–H_2	$H_2\cdots N_3$	$\delta(O_1$–$H_2\cdots N_3)$
HBT-HBZ	S_0	0.996	1.696	147.907
	S_1	1.034	1.563	151.211
	S_1(K)	1.845	1.024	130.796
HBT-HBZ(T)	S_0	0.997	1.682	149.038
	S_1	1.038	1.546	152.365
	S_1(K)	1.841	1.023	130.516
HBT-ClO	S_0	0.998	1.697	147.302
	S_1	1.064	1.498	151.917
	S_1(K)	1.871	1.022	129.870
HBT-ClO(T)	S_0	0.986	1.804	146.192
	S_1	1.022	1.604	149.259
	S_1(K)	2.130	1.011	114.171

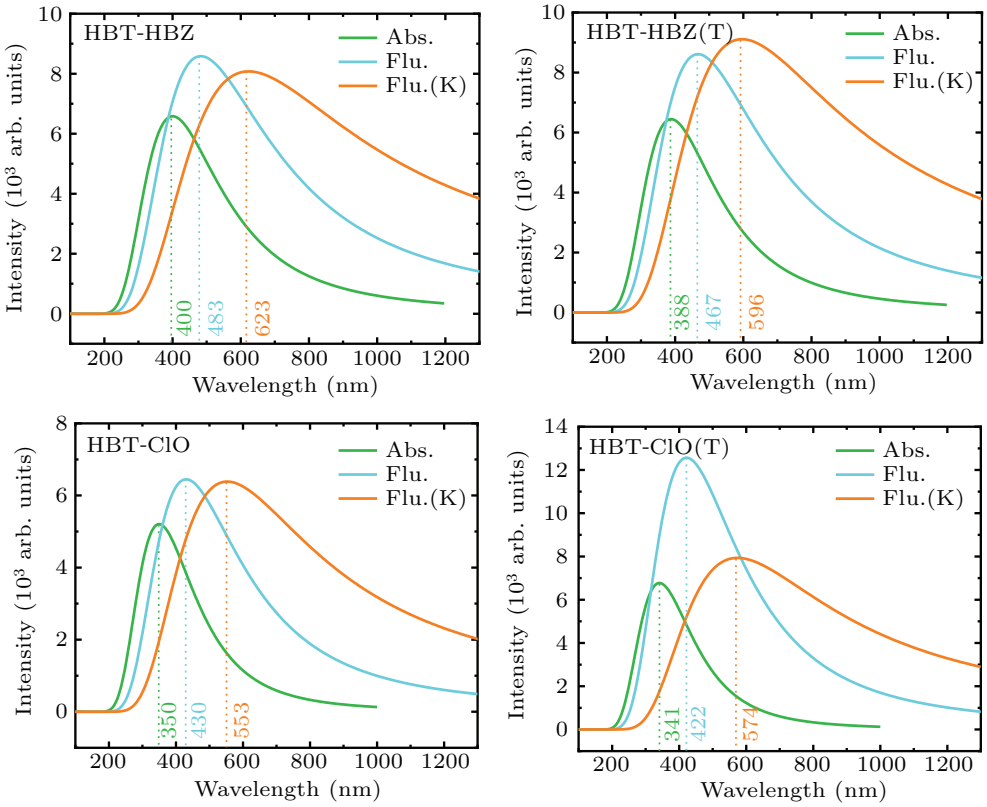


Fig. 3. Calculated electronic spectra of HBT-HBZ, HBT-HBZ(T), HBT-ClO, and HBT-ClO(T) at TDDFT/B3LYP/TZVP/IEFPCM (water) theoretical level.

Table 2. Comparisons of theoretical levels of HBT-HBZ, HBT-HBZ(T), HBT-ClO, and HBT-ClO(T) absorption and fluorescence spectra with experimental data.

Form		Wavelength (nm)	Experimental fluorescence spectra (nm)
HBT-HBZ	Abs.	400	572
	Flu.	483	
	Flu.(K)	623	
HBT-HBZ(T)	Abs.	388	
	Flu.	467	
	Flu.(K)	596	
HBT-ClO	Abs.	350	470
	Flu.	430	
	Flu.(K)	533	
HBT-ClO(T)	Abs.	341	
	Flu.	422	
	Flu.(K)	574	

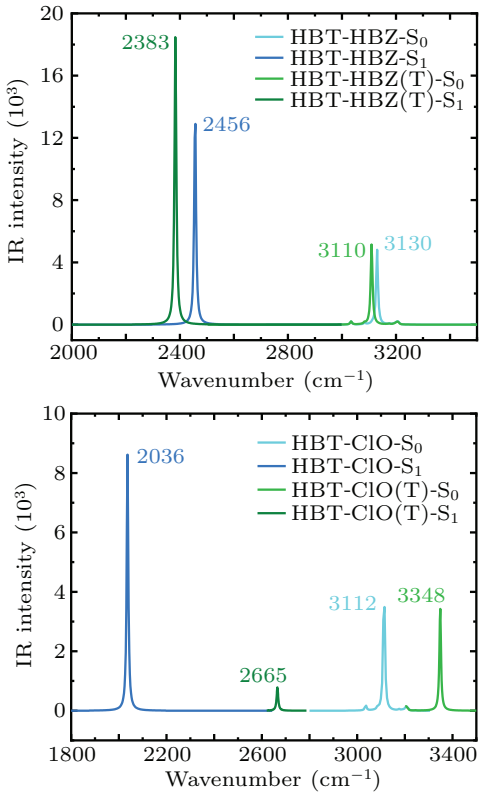


Fig. 4. Calculated infrared (IR) spectra of HBT-HBZ, HBT-HBZ(T), HBT-ClO, and HBT-ClO(T) in spectral region of O_1–H_2 stretching bands.

Typically, the variation of intramolecular hydrogen bonding strength can be reflected by the infrared (IR) vibrational spectra. Under photoexcitation conditions, the spectra are red-shifted in the direction of shorter wavelengths, implying the strengthening of hydrogen bonds. The IR spectra of HBT-HBZ and HBT-ClO and their isomers are shown in Fig. 4. In the S_0 state, HBT-HBZ:3130 cm^{-1} > HBT-HBZ(T):3110 cm^{-1}, HBT-ClO(T):3348 cm^{-1} > HBT-ClO:3112 cm^{-1}. In the S_1 state, HBT-HBZ:2456 cm^{-1} > HBT-HBZ(T):2383 cm^{-1}, HBT-ClO(T):2665 cm^{-1} > HBT-ClO:2036 cm^{-1}. Therefore, the hydrogen bonding of HBT-HBZ(T) is stronger than that of HBT-HBZ, and the hydrogen bonding of HBT-ClO is stronger than that of HBT-ClO(T), too. Furthermore, atoms-in-molecules (AIM) theory[54,55] is used to examine the hydrogen bond characteristics by using the properties of the bond critical point (BCP) position of the hydrogen bond, and the specific results are listed in Table 3. It can be found that the hydrogen bonds are proportional to the molecular dipole moment for both enol- and keto-structures, which means that the dipole moment affects the intramolecular hydrogen bond strength. According to the relative results,[49] the hydrogen bonds in the S_1 state of the enol-structure belong in the strong hydrogen bonds.

Table 3. The energy values of intramolecular hydrogen bonds (ΔE_{HB}) (kcal/mol) and molecular dipole moments (Debye) of HBT-HBZ, HBT-HBZ(T), HBT-ClO, and HBT-ClO(T) in S_1 state. ΔE_{HB} represents hydrogen bond energy.

Name	States	E_{HB} (kcal/mol)	μ (Debye)
HBT-HBZ	S_1	–15.77	2.96
	S_1(K)	–7.41	8.36
HBT-HBZ(T)	S_1	–16.43	3.20
	S_1(K)	–7.52	8.78
HBT-ClO	S_1	–18.69	11.63
	S_1(K)	–6.95	16.63
HBT–ClO(T)	S_1	–13.95	11.17
	S_1(K)	–3.93	14.57

A function of an O_1–H_1 bond length of 0.05 Å is chosen to build a potential energy curve for investigating the ESIPT process of HBT-HBZ and HBT-ClO and their isomers in the S_0 state and S_1 state (Fig. 5). In addition, we also calculate the reaction rate constant k (in unit s^{-1}) of HBT-HBZ, HBT-ClO, and their isomers in the ESIPT process based on Eyring's transition state theory (TST).[52] In the excited state, the activation energy values (energy barriers) for the ESIPT process of HBT-HBZ, HBT-ClO, and their isomers are 0.68, 0.60, 0.05, and 1.84 kcal/mol, respectively (Fig. 5). The Gibbs free energy value of the ESIPT transfer process is 2.41, 2.34, 0.41, and 2.47 kcal/mol, separately, which proves that the ESIPT process is thermodynamically feasible. Based on the thermodynamic equation of TST equivalence, the rate constants of ESIPT processes are calculated to be 2.54×10^{10} (HBT-HBZ), 2.84×10^{10} (HBT-HBZ(T)), 7.40×10^{11} (HBT-ClO), and 2.31×10^{10} (HBT-ClO(T)), respectively, in units kcal/mol/s. Thus, the activity ranking of ESIPT process should follow the order: HBT-HBZ(T) > HBT-HBZ; HBT-ClO > HBT-ClO(T).[56] In summary, the proton transfer rate of HBT-ClO(T) is relatively slow compared with that of HBT-ClO due to its small reaction rate constant, and combined with the properties of the emission peak, HBT-ClO(T) is more favorable for enol-structure exhibiting fluorescent properties. Meanwhile, the energy barrier for reverse proton transfer is too high to overcome, so the keto-structure after proton transfer can exist stably.

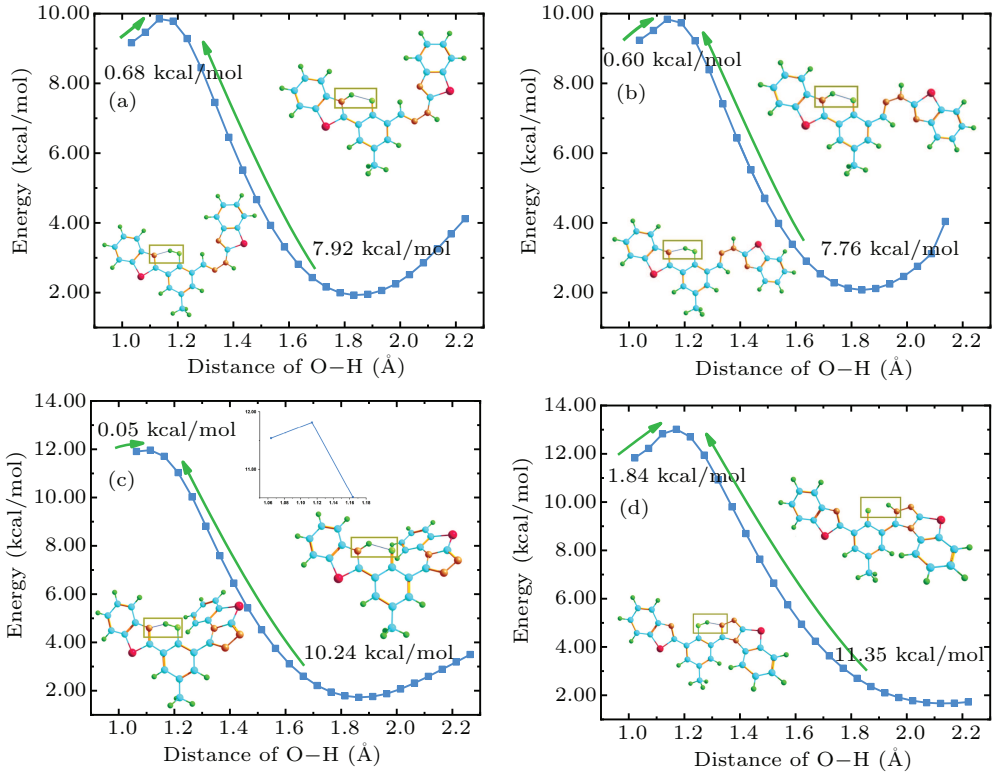


Fig. 5. Potential energy curves of HBT-HBZ, HBT-HBZ(T), HBT-ClO, and HBT-ClO(T) in S_1 state.

The occurrence of the ESIPT process is often accompanied by charge transfer and redistribution. To analyze the intramolecular charge transfer process of HBT-HBZ and HBT-ClO and their isomers, we construct the frontier molecular orbitals (FMOs) as shown in Fig. 6. The oscillator strength, major transition orbitals and CI coefficients of HBT-HBZ, HBT-ClO, and their isomers in different states are shown in Table S2 (see supplementary information).

The MOs distribution of the highest occupied molecular orbital (HOMO) is located mainly in the imine side-chain group and toluene group for HBT-HBZ and HBT-HBZ(T), while the MOs distribution of the lowest unoccupied molecular orbital (LUMO) is located mainly in the benzothiazole group and toluene group. At this point, the molecule exhibits a distinct charge transfer characteristic in the S_1 state, leading to a charge transfer (CT) excitation state. The charge-transfer excitation state will lead to a lower degree of charge coupling, which will result in a lower quantum yield, showing a weak fluorescence or fluorescence quenching. It is consistent with the experimental result that HBT-HBZ exhibits weak orange fluorescence in the S_1 state. For HBT-ClO, in the S_1 state, the MOs distribution of HOMO is located mainly in the imine side-chain group and the toluene group, with a small portion in the benzothiazole group. In contrast, the MOs distribution of LUMO is located mainly in the benzothiazole group and the toluene group, also exhibiting the CT state. Under the enol-structure, the MO distribution of both HOMO and LUMO is located mainly in the benzothiazole group and toluene group without apparent charge transfer phenomena acting as locally excited (LE) state. Moreover, the maximum oscillator strength ($f = 0.9317$) corresponds to the strong cyan fluorescence phenomenon in the experiment. The keto-structure exhibits the CT state due to the apparent intramolecular charge transfer, explaining the HBT-ClO single fluorescence phenomenon. Comparing the FMOs of HBT-HBZ and HBT-ClO and their isomers in the S_1 states, the reason for the difference in fluorescence properties is related to the site of intramolecular hydrogen bond formation.

For the better visualization of the charge transition properties in the S_1 state, "hole–electron" analysis is combined as shown in Fig. 7. The green isosurface (electron) corresponds to the place where the electron density of the excited increases with respect to the ground state, and the blue isosurface (hole) corresponds to the place where the electron density of the excited state decreases in comparison with the ground state. The charge leaving the domain is depicted by combining with the D-index, which describes the distance between the "hole" and the "electron" center of mass. In the S_1 state, the D-index before and after the proton transfer of HBT-ClO are 2.814 Å and 2.255 Å, respectively, and the D-index before and after the proton transfer HBT-ClO(T) are 0.595 Å and 2.130 Å, respectively. This also quantitatively demonstrates that the enol-configuration of HBT-ClO(T) is in the LE state, and the keto-structure is in the CT state, further explaining the single fluorescence. In conclusion, when the system exhibits strong cyan fluorescence, the corresponding molecular structure should be HBT-ClO(T).

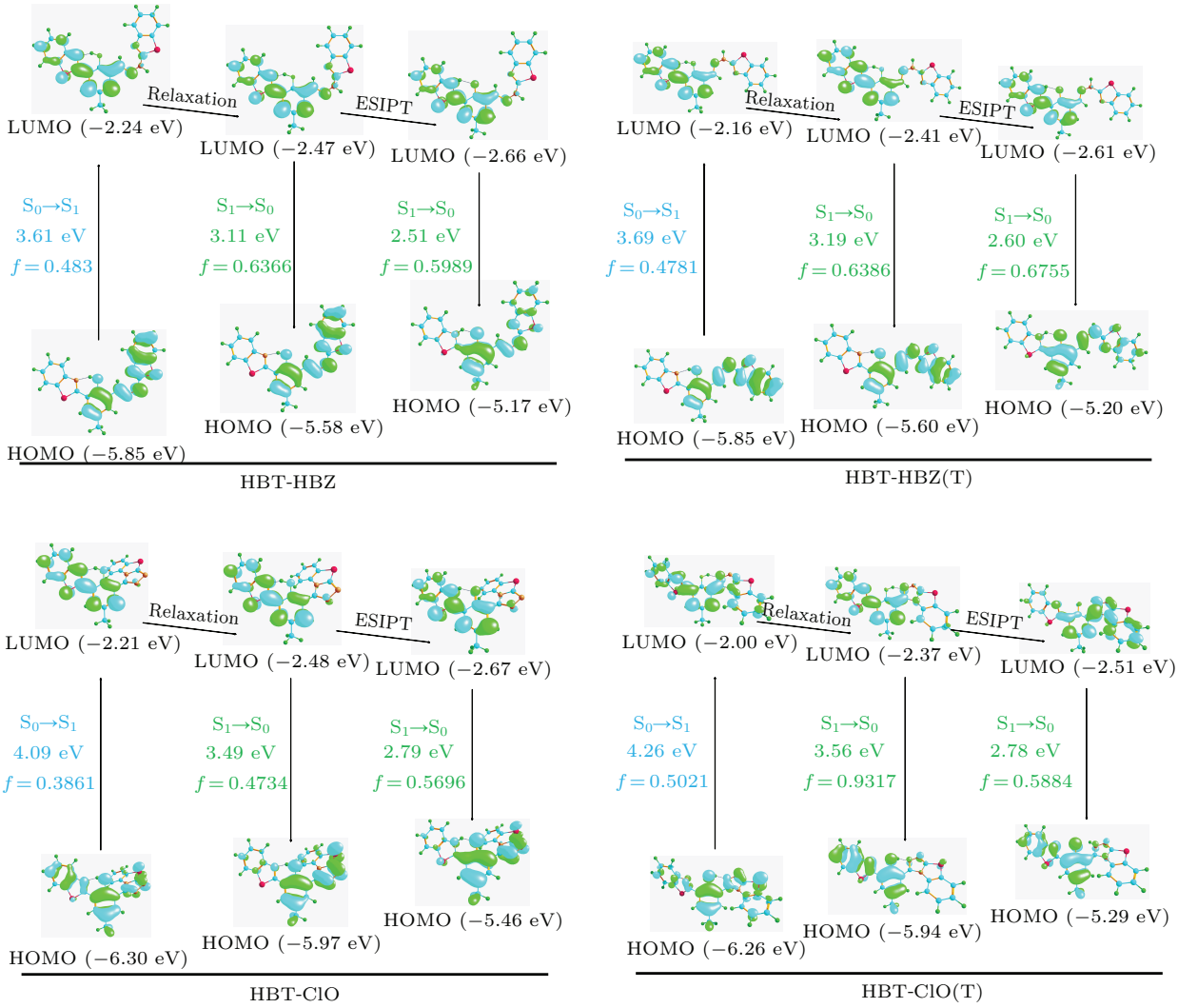


Fig. 6. Frontier molecular orbitals of HBT-HBZ, HBT-HBZ(T), HBT-ClO, and HBT-ClO(T) in S_0 state and S_1 state.

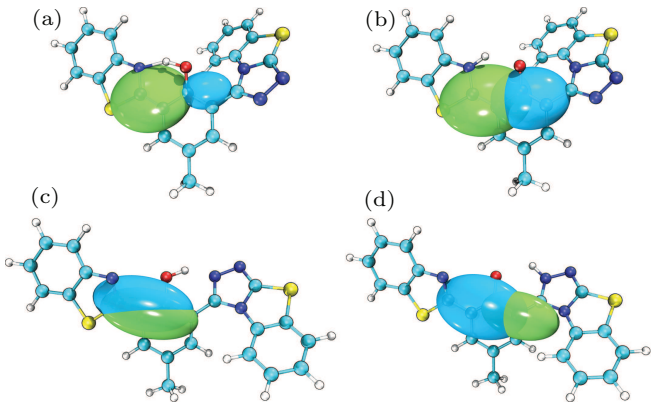


Fig. 7. Hole–electron analysis of (a) HBT-ClO, (b) HBT-ClO(K) , (c) HBT-ClO(T), and (d) HBT-ClO(T) (K) in S_1 state.

Molecular electrostatic potential (ESP) maps are essential for investigating intramolecular electrostatic interactions, predicting reaction sites and molecular properties, and are widely used in many studies. To investigate the ESP properties of HBZ-ClO and HBZ-ClO(T), the ESP on the surface near the relevant atoms in the excited state and the minimum electrostatic potential of the whole system are calculated (Fig. 8 and Table 4). When the ESP on the molecule surface shows blue, it represents a negative electrostatic potential, indicating a tendency to undergo electrophilic reactions.[57] The ESP near the N_1 atom on the benzothiazole group is positive in HBT-ClO. However, the minimal ESP values on the molecular surface are only −6.525 kcal/mol and −0.843 kcal/mol. For HBT-ClO(T), the ESP near the N_2 atom in the triazole group is −23.323 kcal/mol, smaller than that near the N_1 atom in the benzothiazole group (−41.680 kcal/mol). Indeed, it still shows a clear electrophilic nature (−43.373 kcal/mol) and easy to accept protons. Both in HBT-ClO and in HBT-ClO(T), the triazole group has a minimal ESP near the triazole group and exhibits a clear electrophilic property due to the lone pair electrons on the N atoms. In conclusion, the sites of the hydrogen bond in the molecule will have a significant effect on the overall ESP distribution and electron transition of the molecule, which in turn affects the luminescence intensity and fluorescence mechanism.

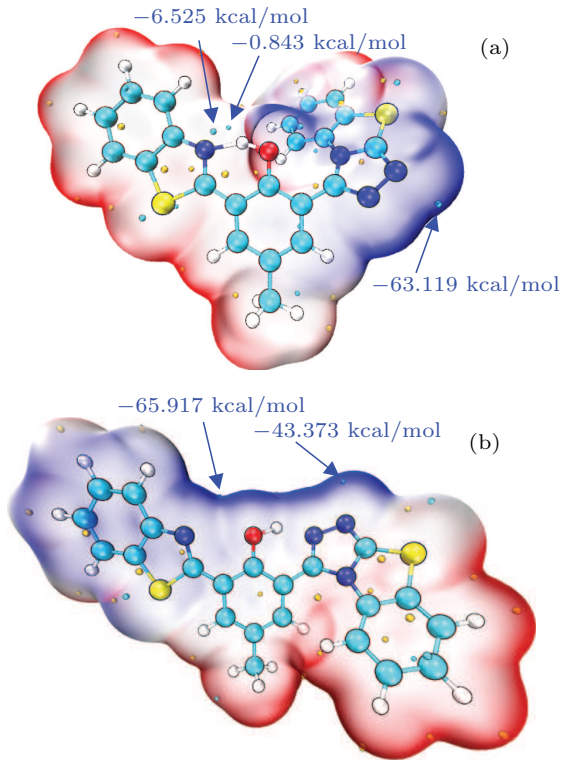


Fig. 8. Molecular electrostatic potential and electrostatic potential minima of HBT-ClO (a) and HBT-ClO(T) (b) in S_1 state.

Table 4. Electrostatic potential on surface of S_1 molecules near HBT-ClO and HBT-ClO(T) atoms.

		All (kcal/mol)	Positive (kcal/mol)	Negative average (kcal/mol)
HBZ-ClO	N_1	2.133	4.912	–2.763
	N_2	–48.021	–	–48.021
HBZ-ClO(T)	N_1	–41.680	–	–41.680
	N_2	–23.323	3.513	–24.443

4. Summary

In this study, the fluorescent mechanisms of HBT-HBZ and HBT-ClO and the corresponding isomers in water samples are explained by theoretical calculation methods based on the B3LYP/TZVP/IEFPCM model. The results of fluorescence spectral analysis reveals that a substantial fluorescence property is exhibited by HBT-ClO(T) in the enol-structure. The results from infrared vibrational spectra and AIM theory demonstrate that the intramolecular hydrogen bonds of HBT-HBZ and HBT-ClO and their isomers are strong in the excited state, and the strength of intramolecular hydrogen bonds is proportional to the dipole moment. The potential energy curves and frontier molecular orbitals show that both HBT-HBZ and HBT-ClO and their isomers are strongly prone to proton transfer in the excited state, and the weak fluorescence of HBT-HBZ and HBT-HBZ(T) in water are due to the significant electron delocalization during photoexcitation, resulting in CT state excitation. Moreover, the corresponding molecular structure should be HBT-ClO(T) when strong cyan fluorescence appears in the solution. The electrostatic potential analyses show that the lone electron pair on the N atom leads to enhanced electrophilicity in the triazole group, increasing the attraction to the proton and favoring the occurrence of proton transfer, which is closely related to the position of the intramolecular hydrogen bond formation. Our contribution demonstrates that the position of intramolecular hydrogen bond formation has a significant effect on the overall electrostatic potential distribution and electron hopping of the molecule, which in turn affects the luminescence intensity and fluorescence mechanism. Above all, our work will provide better theoretical guidance for the probe design, and also help researchers design the fluorescent probes for benzothiazoles better.

Acknowledgement

Project supported by the Open Project of State Key Laboratory of Molecular Reaction Dynamics in Dalian Institute of Chemical Physics (DICP), Chinese Academy of Sciences.

References

[1] Henrique de Araujo T, Okada S S, Ghosn E E B, Taniwaki N N, Rodrigues M R, Rogerio de Almeida S, Mortara R A, Russo M, Campa A and Albuquerque R C 2013 *Cell. Immunol.* **281** 27
[2] Sugiyama S, Okada Y, Sukhova G K, Virmani R, Heinecke J W and Libby P 2001 *Am. J. Pathol.* **158** 879
[3] Steinbeck M J, Nesti L J, Sharkey P F and Parvizi J 2007 *J. Orthop. Res.* **25** 1128
[4] Güngör N, Knaapen A M, Munnia A, Peluso M, Haenen G R, Chiu R K, Godschalk R W L and van Schooten F J 2010 *Mutagenesis* **25** 149
[5] Yap Y W, Whiteman M and Cheung N S 2007 *Cell Signal.* **19** 219
[6] Duan C, Won M, V erwilst P, Xu J C, Kim H S, Zeng L T and Kim J S 2019 *Anal. Chem.* **91** 4172
[7] Zhu L M, Xu J C, Sun Z, Fu B Q, Qin C Q, Zeng L T and Hu X C 2015 *Chem. Commun.* **51** 1154
[8] Huang Y F, Zhang Y B, Huo F J, Liu Y M and Yin C X 2020 *Dyes Pigm.* **179** 108387
[9] Yuan L, Wang L, Agrawalla B K, Park S J, Zhu H, B Sivaraman, Peng J, Xu Q H and Chang Y T 2015 *J. Am. Chem. Soc.* **137** 5930
[10] Wu L, Wu I C, DuFort C C, Carlson M A, Wu X, Chen L, Kuo C T, Qin Y, Yu J, Hingorani S R and Chiu D T 2017 *J. Am. Chem. Soc.* **139** 6911
[11] Li Y A, Yang S, Li Q Y, Ma J P, Zhang S and Dong Y B 2017 *Inorg. Chem.* **56** 13241
[12] Song X, Dong B, X Kong, Wang C, Zhang N and Lin W 2018 *Spectrochim. Acta Part A* **188** 394
[13] Wen H, Huang Q, Yang X F and Li H 2013 *Chem. Commun.* **49** 4956
[14] Majumdar P and Zhao J 2015 *J. Phys. Chem. B* **119** 2384
[15] Wang J, Liu X and Pang Y 2014 *J. Mater. Chem. B* **2** 6634
[16] Xu P F, Liu M H, Gao T, Zhang H L, Li Z W, Huang X Y and Zeng W B 2015 *Tetrahedron. Lett.* **56** 4007
[17] Goswami S, Manna A, Paul S, Das A K, Nandi P K, Maity A K and Saha P 2014 *Tetrahedron Lett.* **55** 490
[18] Chang C C, Wang F, Qiang J, Zhang Z J, Chen Y H, Zhang W, Wang Y and Chen X Q 2017 *Sens. Actuators B Chem.* **243** 22
[19] Yang Y, Qiu F Z, Wang Y Z, Feng Y, Song X R, Tang X L, Zhang G L and W S 2018 *Sens. Actuators B Chem.* **260** 832
[20] Wang J Y, Qu J B, Zhang H T, Wei K and Ni S X 2019 *RSC Adv.* **9** 16467
[21] Nguyen K H, Hao Y, Zeng K, Fan S N, Li F, Yuan S, Ding X J, Xu M T and Liu Y N 2018 *Spectrochim. Acta Part A* **199** 189
[22] He Y H, Xu Y, Shang Y T, Zheng S W, Chen W H and Pang Y 2018 *Anal. Bioanal. Chem.* **410** 7007
[23] Tang L J, Zhou L, Yan X M, Zhong K L, Gao X, Liu X Y and Li J R 2020 *Dyes Pigm.* **182** 108644

[24] Zhao J Z, Ji S M, Chen Y H, Guo H M and Yang, P 2012 *Phys. Chem. Chem. Phys.* **14** 8803
[25] Zhou P W, Hoffmann M R, Han K L and He G Z 2015 *J. Phys. Chem. B* **119** 2125
[26] Hu R, Feng J, Hu D H, Wang S Q, Li S Y, Li Y and Yang G Q 2010 *Angew. Chem. Int. Ed.* **49** 4915
[27] Liu B, Wang H, Wang T S, Bao Y Y, Du F F, Tian J, Li Q B and Bai R K 2012 *Chem. Commun.* **48** 2867
[28] Murale D P, Kim H, Choi W S and Churchill D G 2013 *Org. Lett.* **15** 3946
[29] Xu Z, Xu L, Zhou J, Xu Y F, Zhu W P and Qian X H 2012 *Chem. Commun.* **48** 10871
[30] Zhou P W and Han K L 2018 *Acc. Chem. Res.* **51** 1681
[31] Tang Z, Yang Y F, Yang Y, Wang Y, Tian J and Fei X 2018 *J. Lumin.* **194** 785
[32] Tang Z, Lu, M H, Liu K J, Zhao, Y L, Qi Y T, Wang Y, Zhang P and Zhou P W 2018 *J. Photoch. Photobio. A* **367** 261
[33] Tang Z, Wei H W and Zhou P W 2020 *J. Mol. Liq.* **301** 112415
[34] Zhan H B, Tang Z, Li Z X, Chen X Y, Tian J, Fei X and Wang Y 2021 *Spectrochim. Acta Part A* **260** 119993
[35] Zhao J F and Jin B 2021 *J. Mol. Liq.* **326** 115309
[36] Tao Y P, Han L G, Han Y X and Liu Z J 2016 *J. Mol. Struct.* **1121** 188
[37] Hanaoka K, Kikuchi K, Kojima H, Urano Y and Nagano T 2004 *J. Am. Chem. Soc.* **126** 12470
[38] Wang K J, Xi D Z, Liu C T, Chen Y H, Gu H, Jiang L, Chen X Q and Wang F 2020 *Chin. Chem. Lett.* **31** 2955
[39] Yang X L, He L W, Xu K X, Yang Y Z and Lin W Y 2018 *New. J. Chem.* **42** 12361
[40] Chen W, Yang M, Luo N, Wang F, Yu R Q and Jiang J H 2019 *Analyst* **144** 6922
[41] Li N N, Bi C F, Zhang X, Xu C G, Fan C B, Gao W S, Zong Z A, Zuo S S, Niu C F and Fan Y H 2020 *J. Photoch. Photobio. A* **390** 112299
[42] Wang, C Y, Xu J H, Ma Q J, Bai Y, Tian M J, Sun J G and Zhang Z J 2020 *Spectrochim. Acta Part A* **227** 117579
[43] Frisch M J, Trucks G W, Schlegel H B, *et al.* 2016 Gaussian 16 Revision C.01 (Gaussian, Inc., Wallingford)
[44] Yanai T, Tew D P and Handy N C 2004 *Chem. Phys. Lett.* **393** 51
[45] Schafer A, Horn H and Ahlrichs R 1992 *J. Chem. Phys.* **97** 2571
[46] Cances E, Mennucci B and Tomasi J 1997 *J. Chem. Phys.* **107** 3032
[47] Cammi R and Tomasi J 1995 *J. Comput. Chem.* **16** 1449
[48] Miertuš S, Scrocco E and Tomasi J 1981 *Chem. Phys.* **55** 117
[49] Grimmea S, Antony J, Ehrlich S and Krieg H 2010 *J. Chem. Phys.* **132** 154104
[50] Lu T and Chen F W 2012 *J. Comput. Chem.* **33** 580
[51] Liu Z Y, Lu T and Chen Q X 2020 *Carbon* **165** 461
[52] Lu T, TST calculator, http://sobereva.com/310 (accessed 8 17, 2021)
[53] Fernández-Ramos A, Ellingson B A, Meana-Pañeda R, Marques J M C and Truhlar D G 2007 *Theor. Chem. Account.* **118** 813
[54] Emamian S, Lu T, Kruse H and Emamian H 2019 *J. Comput. Chem.* **40** 2868
[55] Tang W, Sanville E and Henkelman G 2009 *J. Phys.: Condens. Matter* **21** 084204
[56] Yang Y F, Luo X, Ma F C and Li Y Q 2021 *Spectrochim. Acta Part A* **250** 119375
[57] Hunt P A, Kirchner B and Welton T 2006 *Chem. Eur. J.* **12** 6762